FULL RESEARCH ARTICLE

Influence of print settings on conductivity of 3D printed elastomers with carbon-based fillers

Alexandra Glogowsky[1] · **Michael Korger[1]** · **Maike Rabe[1]**

Abstract

Flexible, elastomeric materials for 3D printing have attracted considerable interest due to their potential application in clothing, shoe manufacturing and orthopedics. At the same time, smart clothing is also moving closer to more mainstream applications; as such, it is of considerable interest to combine both the structural and smart functions 3D printing offers in one material. While smart functionalities may be incorporated in a textile in a variety of ways (e.g. using shape-memory polymers), the use of electronic components such as sensors and actuators allow smart response to a multitude of stimuli. This necessitates the use of conductive and flexible materials that offer reliable conductivity after printing and provide optically attractive results. It is known that print conditions influence electrical properties, but while the print parameters are well researched for hard materials, there is not as much research for flexible compounds. Here, we show the influence of print speed, temperature, infill orientation, layer thickness and print mode (i.e. time between printing of successive layers). It was found that the most influential parameters are print mode, infill orientation and print temperature. The differences in electrical properties between the three materials used in this test may be explained by differences in filler content. A preliminary study into the optimization of the shape of a printed conductive line on elastic textile shows that the overall length of the printed path needs to be adapted to the maximum stretch of the textile, while shape has little influence on conductivity.

Keywords 3D printing · Elastomers · Conductive thermoplastics

1 Introduction

3D printing has been established in many fields, not only as a prototyping technique, but is increasingly used for one-off production of high-value products such as prosthesis, orthopedics and shoes. 3D printing offers the possibility of producing customized, digitally prepared products for technical and clothing applications both as stand-alone products and in combination with textiles. It has been shown that textile-polymeric composites produced via 3D printing are durable and adaptable to a variety of applications, e.g. by utilizing soft-touch materials in close-to-the-body applications or compounds containing flame retardants for technical applications [1, 2]. Smart textiles have gone through a similar process of increasing industrial and customer acceptance with a multitude of products being available on the market today. To produce electrically conductive paths, screen-printing of conductive pastes [3–5] as well as the utilization of conductive threads through embroidery, weaving or knitting are common [6–8]. Elastomeric, conductive materials have been used as strain sensors for smart textile applications [9, 10]. While electrically conductive 3D printing compounds of hard materials (e.g. polylactic acid [11–15], acrylonitrile butadiene styrene [12, 15, 16]) are well researched, relatively little research into conductive elastomeric materials is available. Hohimer et al. investigated compounds of thermoplastic polyurethane (TPU) and multi-walled carbon nanotubes printed with a filament printer. They found a positive correlation between increased layer height and conductivity, attributed to reduced formation of interfacial barriers and a

✉ Alexandra Glogowsky
  alexandra.glogowsky@hs-niederrhein.de

  Michael Korger
  michael.korger@hs-niederrhein.de

  Maike Rabe
  maike.rabe@hs-niederrhein.de

[1] Research Institute for Textile and Clothing, Hochschule Niederrhein-University of Applied Sciences, Webschulstr. 31, Mönchengladbach 41065, Germany

slight increase in conductivity due to increased print temperature. The formation of internal voids is cited as the reason for the negative impact on conductivity due to poor formation of conductive networks [17]. Georgopoulou et al. compared single extruded filaments of the same commercially available TPU compound used in this paper (Eel by NinjaTek) and a blend of styrenic block copolymer (TPS) and carbon black regarding their strain-sensing capabilities [10]. Eutionnat-Diffo et al. prepared a flexible conductive filament by following a different approach to blending immiscible polymers with conductive fillers to achieve selective location of fillers in one phase/the interface of the blended polymers [18, 19]. Tzounis et al. explored the application of TPU/carbon nanotube composites as thermoelectric materials and measured conductivity of printed samples (without appplying stress to the samples) as well [20]. Xiang et al. investigated 3D-printed TPU / carbon nanotube composites for their strain-sensing abilities and found that modification with 1-pyrenecarboxylic acid improved tensile and electrical properties through enhancement of interfacial properties [21]. Resistivity could be further reduced by inclusion of silver nanoparticles [22].

So far, there has been little research into printing with granulate-based 3D printers, even though this technique is optimally suited to printing with soft materials and offers the possibility to print materials that are otherwise hard to print. Furthermore, the effect of printing these conductive, elastomeric materials directly on a textile is yet to be determined; with that, properties during the use and care of a textile also have to be investigated. Another aspect investigated in this paper is the behavior of conductive, 3D printed samples under stress. In this paper, we present the influence of print parameters on two commercially available, flexible conductive materials as well as one custom blend of TPU and multi-walled carbon nanotubes during granulate printing. The influence of different undulation patterns on conductivity under stress is also described.

2 Materials and methods

2.1 Materials

Three materials are compared regarding their electrical properties: the widely available "Eel" (purchased from NinjaTek/Fenner Inc.), which is a TPU containing < 18% carbon black, a masterbatch composed of TPU-type GPU FPU 89A AF from Covestro with 15% multiwall carbon nanotubes (MWCNTs), which was manufactured as a custom blend by Nanocyl SA. and is called TPU15CNT for the purpose of this paper, and a conductive material based on TPS from Kraiburg TPE GmbH & Co. KG called Thermolast K TC8OEX. Eel has a hardness of 90 Shore A, while TC8OEX is softer at 83 Shore A, making them ideal for application in clothing that may be worn close to the body. TPU15CNT has a comparable hardness to Eel.

2.2 Printing

All samples are produced on a granulate printer (PAM Series P from Pollen AM Inc. with 0.4 mm nozzle). Initial print settings are chosen to obtain optically good prints (even surface quality, no gaps, good layer adhesion); differences between "standard" settings for both materials are displayed in Table 1. Standard sample size is 60 mm × 2 mm × 1 mm (L × W × H).

2.3 Testing

Resistance R is measured using a milliohmmeter (Resistomat 2316 from Burster Präzisionsmesstechnik GmbH & Co. KG) and a sample clamp that allows reproducible clamping pressure and clamping distance. To minimize the influence of contact resistance, the ends of the samples are dipped in silver ink (Auromal 38 from Deduco); all samples are climatized for > 24 h at 20 °C/65% r.H. prior to testing. The cross-sectional area A of each individual sample is determined by cutting it in half using a scalpel and measuring A

Table 1 "Standard" settings, if not explicitly stated otherwise

	Layer thickness in µm	Temperature nozzle/screw in °C	Print mode	Print speed in mm/min	Infill direction (s. Fig. 3) in °
Eel	100	180/210	ObjectByObject	2400	45/− 45 (2 outlines)
TC8OEX	200	210/220			
TPU15CNT	200	180/215			

Note: It was not possible to achieve satisfactory print results for Eel at a layer height of 200 µm. This is reflected in the difference in standard print settings

microscopically around the perimeter of the sample (Keyence VHX600); small internal voids are ignored. For the reference measurements on filaments, A is calculated from the diameter, measured with calipers. The volume resistivity ρ of the sample is calculated according to Eq. 1 with the resistance R measured by choosing a measuring distance of $l = 50\ mm$. The number of samples prepared are $n = 5$ ($n = 10$ for reference measurements on filaments).

$$\rho = R \times \frac{A}{l} \tag{1}$$

2.4 Variation of shape

To test the influence of different undulation patterns on the conductive properties of the print, the best setting for material TC8OEX is used to print shapes (s. Table 3), both with and without textile. A sine wave is used as the model for undulating shapes, with a width of 2 mm and a printed height of 1 mm. The shape of the wave is modified to enable facile positioning of the sample in the measuring clamp (s. Eq. 2); in addition to the sine wave, a zigzag pattern (s. Eq. 3) and a step function (s. Eq. 4) with corresponding parameters are realized. The number of samples prepared is $n = 5$.

$$f(x) = a \times sin(b \times x) \tag{2}$$

$$g(x) = \frac{2a}{\pi} \sin^{-1}(\sin(b \times x)) \tag{3}$$

$$h(x) = a \times \mathrm{sgn}(a \times (\sin(b \times x)) \tag{4}$$

The factors a and b are chosen according to Table 2; the extrema of all shapes are located at a multiple of 50 mm, which is the initial clamping distance of all samples. The

actual length of the conductive material at a clamping length of 50 mm is also given in Table 2. For a graphical representation of the influence of the variation of shape, amplitude and frequency, s. Fig. 1.

The same shapes are printed directly onto a knit fabric in the course and wale direction to determine the influence of fabric elasticity on the conductivity of the print. The textile used in all experiments is a double jersey knit, composed of 94% meta-aramide and 6% elastane. The fabric has 21 wales/cm, 10.5 courses/cm and a thickness of 0.42 mm, as measured with a micrometre screw simulating nozzle pressure. This fabric is selected for the experiments, as previous investigations have shown various TPU and TPS materials to have good adhesion to this fabric [2]; furthermore, the combination of knit structure and elastane give the fabric high elongation with good recovery. Before printing, the fabric is fixed in a relaxed state (i.e. without pre-stretching) on the print bed using double-sided tape. To account for the thickness of the fabric during printing, the distance between nozzle and print bed (z-offset) is increased by the measured thickness of the textile.

For all samples, resistance is tested in the same way described above, without previous stresses to the sample. For the samples that are directly printed on the textile, only one side of the clamp touches the print. An influence of one-sided clamping on resistance was ruled out (repeated measurement of samples clamped from both sides and with one side of the clamp insulated). The initial clamping distance of 50 mm is increased in steps of 5 mm without removing the sample, to a maximum clamping distance of 100 mm. The number of samples prepared is $n = 5$. Only the first stress to the material is recorded in this study.

Table 2 Systematic variation of sample shape through variation of amplitude and frequency of undulation

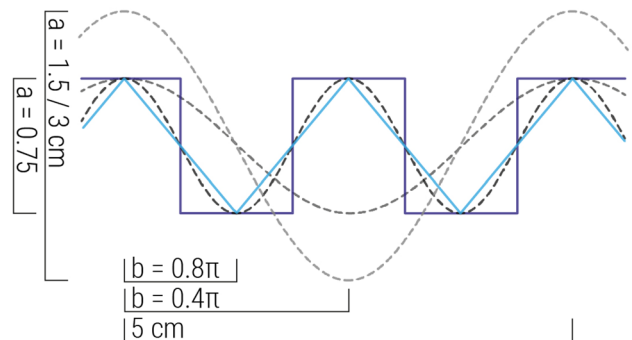| Shape	Factor a	Factor b	Actual length at 50 mm clamping length in mm
Sine	1.5	0.2 π	60
Sine	1.5	0.4 π	81
Zigzag			78
Step			110
Sine	0.75	0.4 π	60
Zigzag			58
Step			80
Sine	0.75	0.8 π	81
Zigzag			78
Step			110

Fig. 1 The influence of the variation of factors a and b (amplitude and frequency) in Eqs. 2, 4, 3 is shown in dashed lines, influence of the variation of shape is shown in blue

3 Results

3.1 Printing parameters

Reference measurements on the raw material filaments are listed in Table 3.

3.1.1 Infill angle

In the first step, the infill angle is varied, with 45°/−45° being the standard setting for functional printing, while 0° represents a crosswise direction of the infill and 90° a lengthwise direction. For 0° and 90° infill, all layers of the print follow the exact same print lines, while the direction of the infill pattern alternates between layers for the 45°/−45° infill. This is illustrated in Fig. 2.

The results of this series are shown in Fig. 3. Prints with TC8OEX and a 90o infill are mechanically unstable and result in split layers. These samples cannot be tested; a variation of print mode does not improve this outcome. While results are inconclusive for TC8OEX, Eel and TPU15CNT show statistically significant differences at a significance level of 5% ($\alpha > 0.05$) of resistivity as a function of infill orientation. As expected, the lengthwise infill direction results in the lowest resistivity values. While the difference between 0° and 45° infill is not significant for TC8OEX, for Eel and TPU15CNT, this difference in the infill angle leads to improved conductivity. It is therefore preferable to use an infill pattern that follows the direction of the current flow, if possible. In cases where mechanical stability is insufficient with this technique, a diagonal infill pattern should be used.

3.1.2 Print speed and print mode

The parameters print speed and print mode are investigated in one combined experiment. The difference between the print modes LayerByLayer and ObjectByObject printing is the time to cool before the next layer is printed: five samples are printed in one print job, but for ObjectByObject mode the individual sample is printed as one (i.e. the next layer is printed before the material underneath has had much time to cool), while LayerByLayer mode means the first layers of all five samples are printed before the second layers are printed on top (i.e. the first layer has had time to cool). Time to cool is, of course, also influenced by print speed and the mass of material extruded (i.e. nozzle size and layer thickness) and can be influenced externally by cooling with a fan (this function was disabled for all prints). While print speed and nozzle size are the same for all samples, layer thickness varies, with TC8OEX and TPU15CNT at 200 μm and Eel at 100 μm. According to results shown in Fig. 4, it is not possible to deduct an influence of print speed (no significant differences between resistivities for TC8OEX and TPU15CNT, with the only significant difference found between Eel at 1600 mm/min and 2400 mm/min; $\alpha > 0.05$); as higher speed does not have a pronounced *negative* effect on conductivity it is preferable to print at higher speeds to achieve faster production. While the difference between print modes for TC8OEX (s. also Fig. 3) and TPU15CNT is not significant

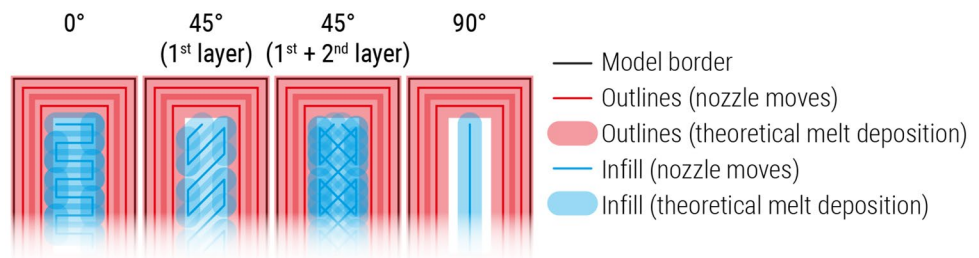Fig. 2 Graphical representation of selected infill angle orientations (to scale)

Fig. 3 Resistivity of samples of materials TC8OEX (left), Eel (middle) and TPU15CNT (right) printed using different angles for the infill of the samples
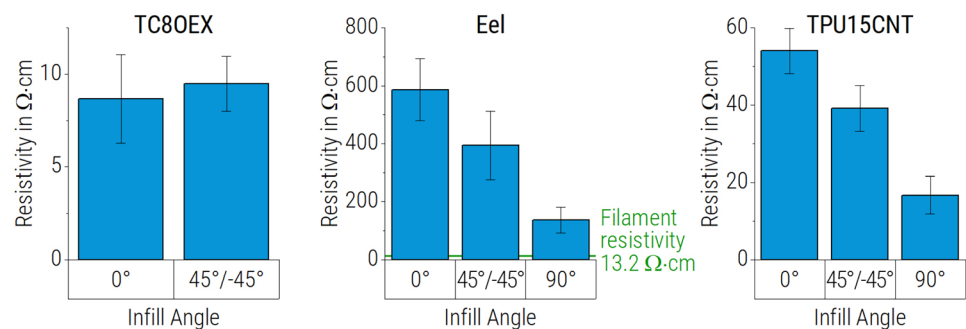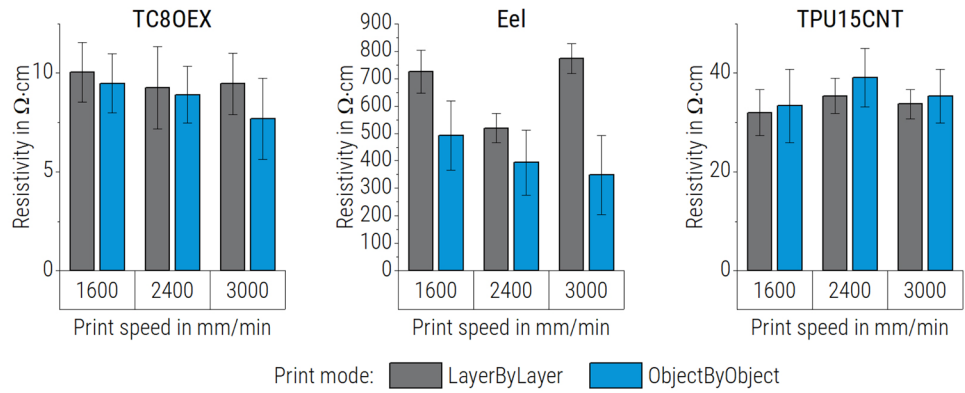
Fig. 4 Resistivity of samples of materials TC8OEX (left), Eel (middle) and TPU15CNT (right) printed using different print speeds and print modes

(α >0.05), Eel again shows more pronounced differences. The fact that both settings only show a significant influence on the Eel samples might be due to the thinner layers in the Eel series. As less material is applied in one layer, the material cools down faster, so that the small improvements achievable by variation of print speed and print mode have a higher impact in this case. Furthermore, the cross sections of samples printed in ObjectByObject mode show less faults and better melting of the layers, resulting in better mechanical properties.

3.1.3 Layer thickness

The third factor under investigation is layer thickness. In general, layer thickness has an influence on dimensional accuracy (in z-direction of printing) and optical evenness; while thinner layers provide better print quality, the production time of the sample increases. Layer thickness is also selected according to the print nozzle used; in general, the minimum layer thickness is dictated by the accuracy of the print bed axis, while the maximum layer thickness is around 60% of the nozzle diameter (this is a geometric limitation as the extruded material needs to be pressed into the print surface/previous layers to achieve adhesion). While the differences between resistivities in our trials are not significant for TC8OEX and Eel, TPU15CNT shows a more pronounced

influence of layer height on resistivity ($\alpha > 0.05$). While the non-significant results of TC8OEX and Eel make it impossible to come to a general conclusion, the positive influence of thicker layers for TPU15CNT cannot be ignored (s. Fig. 5). For the purpose of printing conductive paths on a smart textile, where simple shapes predominate, it is preferable to sacrifice some accuracy in favor of speed. As fewer and thicker layers will presumably also result in less internal voids and—in reversion to the assumption above—cool down slower, printing thicker layers is preferable.

3.1.4 Print temperature

Finally, temperature is investigated as a factor in achieving optimal conductivity. The high variations in temperature shown here (from 200–240 °C) are only feasible on a granulate printer because the material is pressed through the nozzle using a screw. It is not possible to print TC8OEX on a standard filament printer and Eel can only be printed at > 220 °C in filament form, as the mechanism that feeds the material into the print head of standard printers relies on a relatively stiff filament to push the melt through the nozzle, making it challenging to print flexible materials. While the results are not statistically significant for TC8OEX and Eel, TPU15CNT shows a positive influence of increasing print temperatures on conductivity ($\alpha > 0.05$). While it is

Fig. 5 Resistivity of samples of materials TC8OEX (left), Eel (middle) and TPU15CNT (right) printed using different layer thicknesses
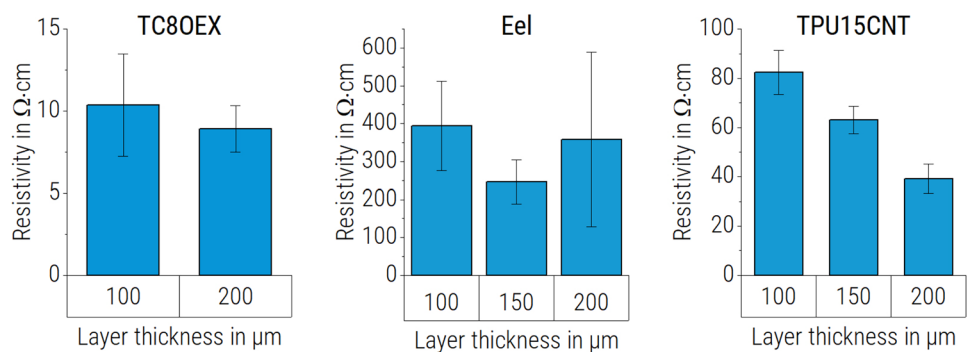
Fig. 6 Resistivity of samples of materials TC8OEX (left), Eel (middle) and TPU15CNT (right) printed using different temperature settings: the difference between screw and nozzle temperature is kept constant
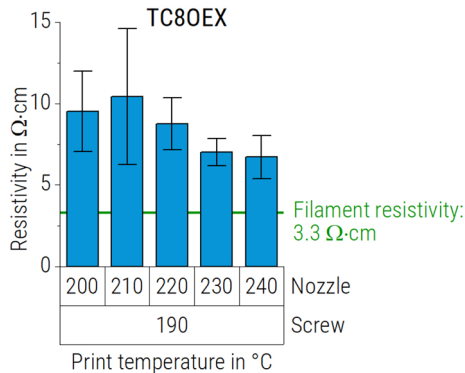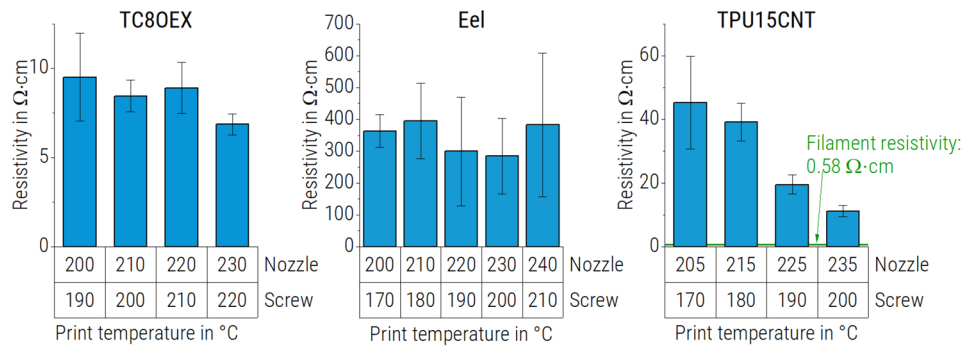

Fig. 7 Resistivity of TC8OEX samples printed using different temperature settings: only the nozzle temperature is increased

not clear from the results shown in Fig. 6 whether a linear dependence between increasing print temperature and lower resistivity exists, the highest print temperature achieved the best conductivity for TC8OEX and TPU15CNT. The very high standard deviation for the highest print temperature of Eel may be a result of mechanical damage to the sample, as the print gets more brittle due to temperature damage during printing. As all materials give the best print quality results at different temperatures (10 °C difference between screw and nozzle temperatures for TC8OEX vs. 30 °C for Eel and TPU15CNT), it is hard to come to general conclusions.

It is generally preferable to print at lower temperatures and minimize temperature damage deriving from very high extrusion temperatures. For this reason, it is also investigated

whether similar results can be achieved by increasing only the nozzle temperature and thus limiting thermal damage to the polymer during the residence time in the screw section of the extruder (most TPU and TPS types are processed < 220 °C [23]). Figure 7 shows that this strategy still yields similar results, though the differences between the results shown in Fig. 7 are not significant. The lowest resistivity was again achieved using the highest temperature for the nozzle (the trial at 190 °C screw temperature/240 °C nozzle temperature was the lowest resistivity achieved overall). When the results in Fig. 7 are compared to the results from the previous experiment (varying screw temperatures with the nozzle temperatures, shown in Fig. 6—TC8OEX) the differences between samples printed at the same nozzle temperature are also not significant. Regarding temperature it is therefore possible to conclude, that firstly, increased processing temperature is conducive to achieving lower resistivity and secondly, that it is sufficient to increase nozzle temperature without increasing screw temperature as well.

The print settings used to achieve the lowest resistance in this series are listed in Table 3 with the conductivity before printing also given. For comparison, the reference measurements of resistivity on filaments are given in Fig. 3 (Eel, 90° infill angle), Fig. 6 (TPU15CNT, 235 °C nozzle temperature) and Fig. 7 (TC8OEX, 240 °C nozzle temperature). It is clear that Eel and TPU15CNT have much higher resistance after printing, even if the print conditions are optimal (by a factor of ~ 10 (Eel) and ~ 19 (TPU15CNT)); TC8OEX only has slightly higher resistance after printing (increase by a factor of ~ 2). Furthermore, for Eel and TPU15CNT, resistivity

Table 3 Print settings used to achieve the best conductivity in the series all materials

	Layer thickness in µm	Temperature nozzle/screw in°C	Print mode	Print speed in mm/min	Infill direction in°	Lowest resistivity in Ω cm	
						Before printing (on filament)	After printing
Eel	100	180/210	ObjectByObject	2400	90	13.2	137.2
TC8OEX	200	190/240			45/− 45	3.3	6.7
TPU15CNT	200	200/235			45/− 45	0.58	11.2

appears to be more susceptible to changes in the print parameters (means ranging from ~ 137 Ω cm to 774 Ω cm for Eel, from 11.2 Ω cm to 82.5 Ω cm for TPU15CNT, compared to a range from only 6.7 Ω cm to 10.4 Ω cm for TC8OEX). This might be due to differences in filler content, as contact between conductive fillers is less likely to be negatively influenced if a high filler content is present thus leading to a more stable resistivity values, even if print conditions are not optimal (as also described by Hohimer et al. [17]). Hampel et al. compared two different rigid materials and found a very high coefficient of variation of up to 30% for resistivity of the less conductive material, even when using the same parameters [15]. This is also reflected in our experiments, with acceptable coefficients of variation for resistivity of < 20% achieved in 36% of experiments with Eel, compared to 77% and 63% of experiments with TPU15CNT and TC8OEX, respectively.

In the last step, the sample dimension is varied. As resistivity is a material parameter and should be independent of sample dimensions, the results displayed in Fig. 8 show more variation than expected. However, there are very little statistically significant differences between the samples. One difference is found for the variation of sample thickness in Eel (between 400 μm and 1000 μm thickness), another for the sample width of TPU15CNT (the 4 mm wide sample has a significantly higher resistivity than the 2 mm and 3 mm wide samples). As both differences only appear in one material type, it is not possible to draw any conclusions. Some technical limitations in 3D printing might have an influence, such as the two "outlines" that are needed for printing. These outlines follow the shape of the model used for printing (s. Fig. 3 for a graphical representation of the outlines in these prints) and are therefore printed in the same direction as a 90°-infill. In the wider samples, the influence of the infill dominates over the influence of the 90°-outlines, which might explain a higher resistivity of wider samples as seen in TPU15CNT. As no such correlation can be found for TC8OEX or Eel, a general statement regarding the optimization of the dimensions of a conductive path cannot be made at this point.
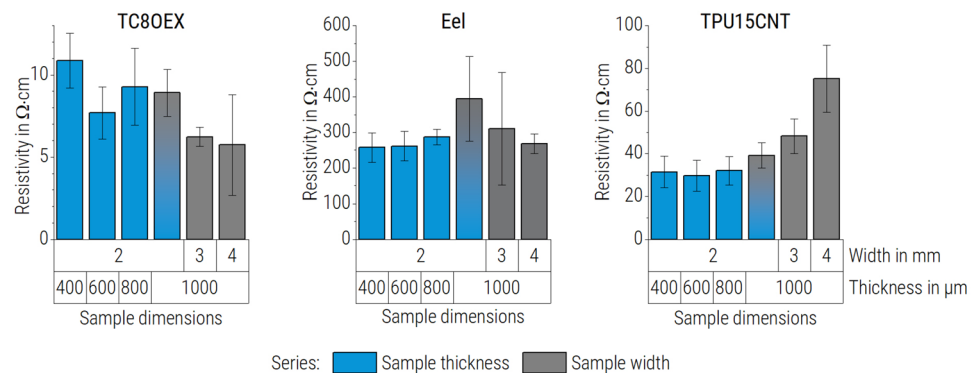
3.2 Variation of shape

3.2.1 Print without a textile

For the investigation of undulating shapes, the amplitude and frequency of the sine wave are varied (factors *a* and *b* in Eqs. 2, 3 and 4, respectively) as well as the general shape (s. also Fig. 1). Only material TC8OEX is further investigated, as it shows the lowest resistivity overall. The best print setting (s. Table 3) is used for all further prints. Figure 9 shows the increasing resistance relative to the elongation (defined here as the change in clamping distance relative to the initial clamping distance of 50 mm, i.e. 20% elongation corresponds to a clamping distance of 60 mm, irrespective of the actual length of material clamped at the start of the test). Figure 10 displays the same data, plotted against the clamping distance relative to the actual printed length of the sample (s. Table 2 for sample length). Both Figs. 9 and 10 show the first elongation of the samples, without previous strain. As resistance is displayed, not resistivity, the initial resistance of the sample depends mainly on the actual length of the material that is clamped. Step functions result in the highest resistance (samples with the longest actual length), while sine and zigzag samples are very close in length (zigzag samples are ~ 4% shorter than sine samples) and thus have very similar overall resistance. The straight sample shows an immediate increase in resistance, followed by a non-linear increase with further stretching. In Fig. 9 it is obvious that all other samples tested initially show an area with little change in resistivity. For each shape, this amount of stretching is about as long as the additional length achieved by printing the undulating shape (s. Table 2). This can be seen much better in Fig. 10: the first noticeable changes in resistance occur shortly before the sample is fully stretched (at ~ −10% elongation relative to the actual sample length), major changes in resistance occur once the shape is fully stretched out and the material starts to be strained (i.e. 0% elongation relative to the actual sample length). Resistance is not influenced by the amplitude or frequency of the sample shapes but is mainly dependent on sample length.

Fig. 8 Resistivity of samples of materials TC8OEX (left), Eel (middle) and TPU15CNT (right) printed using different sample dimensions

Fig. 9 Resistance of samples printed with TC8OEX; influence of changes in shape and undulation pattern and stetched along the *x*-axis. Elongation is displayed as the change in clamping distance relative to the initial clamping distance of 50 mm
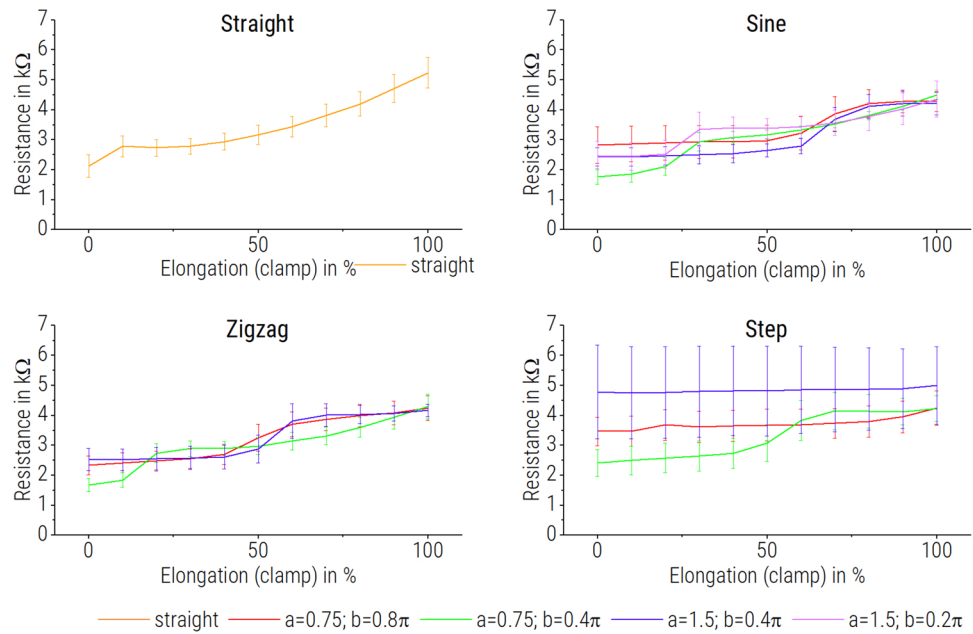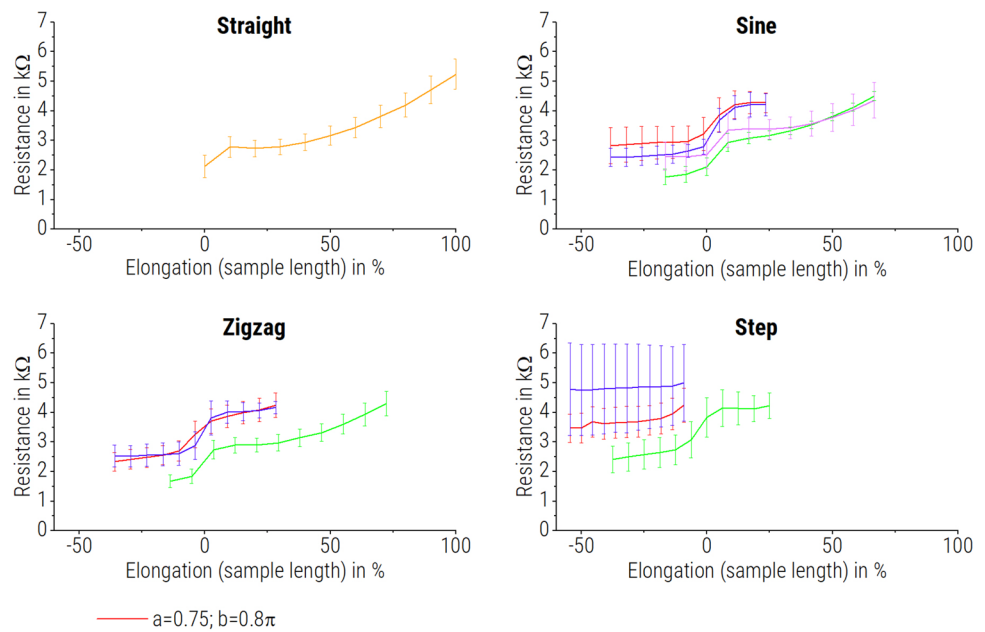
Fig. 10 Resistance of samples printed with TC8OEX; influence of changes in shape (sine, zigzag, step function) and undulation pattern (amplitude and frequency) and stretch along the *x*-axis. Elongation is displayed as the change in clamping distance relative to the actual length of the clamped material as listed in Table 2

This is most obvious in Fig. 10, as the sine and zigzag samples with the factors $a = 0.75; b = 0.8\pi$ and $a = 1.5; b = 0.4\pi$ have the same length overall and therefore behave extremely similar when stretched. A comparison between sine and zigzag shape reveals no major differences regarding their response to strain.

3.2.2 Print on textile

The next step towards investigating conductivity dependent on strain for smart textile use is 3D printing the conductive polymer on an elastic fabric. Depending on the fabric properties, the print cannot stretch uniformly in the direction of the stress applied but is constrained by the fabric to which it is permanently fixed, resulting in uneven elongation along the print path. This is shown in Fig. 11. Some samples slip out of the clamps before the maximum clamping distance of 100 mm is achieved, especially samples printed in the wale direction, as the textile is less elastic in this direction. In all cases, the prints adhere well to the textile and do not peel off during the elongation of the sample.

Fig. 11 Uneven elongation of sample step $a = 0.75$; $b = 0.4\pi$ printed in course direction; some wales are marked to demonstrate stretching pattern


The results of the experiment are displayed in Fig. 12 (only shapes of the same overall length are shown, so the effect of amplitude and frequency may be adequately compared). In all cases, the resistance of samples printed on fabric is higher than that of those not printed on fabric by a factor of ~ 2. The print direction appears to influence the electrical properties of the composite. This directional influence is highest when only a straight line is printed and least apparent in the step shape. This makes sense, because in each step shape, 50 mm of the shape is printed in one direction and 60 mm in the other, i.e. all sections of the printed shape strictly follow the wale or course direction. For the sine function prints, the resistance was higher when printed in the course direction, while the opposite was true for the zigzag function prints; there is no clear cause of this behavior, as both shapes have a balanced proportion of the print in each direction. The difference in overall resistance appears to be an effect of printing, as the initial values of resistance (at 50 mm clamping distance) are different. This might be due to the surface structure of the textile or the deformation of the textile during printing, as the print head touches the fabric surface during printing. Furthermore, adhesion to the fabric is mainly

due to the physical interaction between the polymer and the fabric (i.e. the melt penetrating the fabric and cooling around the fibers) [24–26]. This means that adequate adhesion is only achieved when at least the first printing layer penetrates into the fabric, leading to a high amount of voids and fibers that do not contribute to conductivity.

Another difference between the samples with and without fabric attached is the response to elongation below 0% elongation (when strain is mainly applied to the shape, not the material itself), as seen in Fig. 12. A gentle increase in resistance can be noted here in all samples printed on fabric, while the samples without attached textiles show a steady resistance until about -10% elongation. This is most apparent in zigzag samples in both directions as well as the sine sample printed in the wale direction. Due to the uneven distribution of strain along the fabric (Fig. 11) it is possible that some areas of the conductive material are stretched less than others (i.e. more strain on the horizontal than the vertical components of the shapes), leading to a more gradual increase in resistance with gradual elongation, visible as the slope of the resistance curve in Fig. 12. This hypothesis is further strengthened as the sine and zigzag samples printed in wale direction (in which the textile has lower elongation

Fig. 12 Resistance of samples printed with TC8OEX directly on fabric and comparison with corresponding samples from Fig. 10; influence of changes in shape (sine, zigzag, step function) and undulation pattern (amplitude and frequency) and being stetched along the *x*-axis. Elongation is displayed as the change in clamping distance relative to the actual length of the clamped material as listed in Table 2
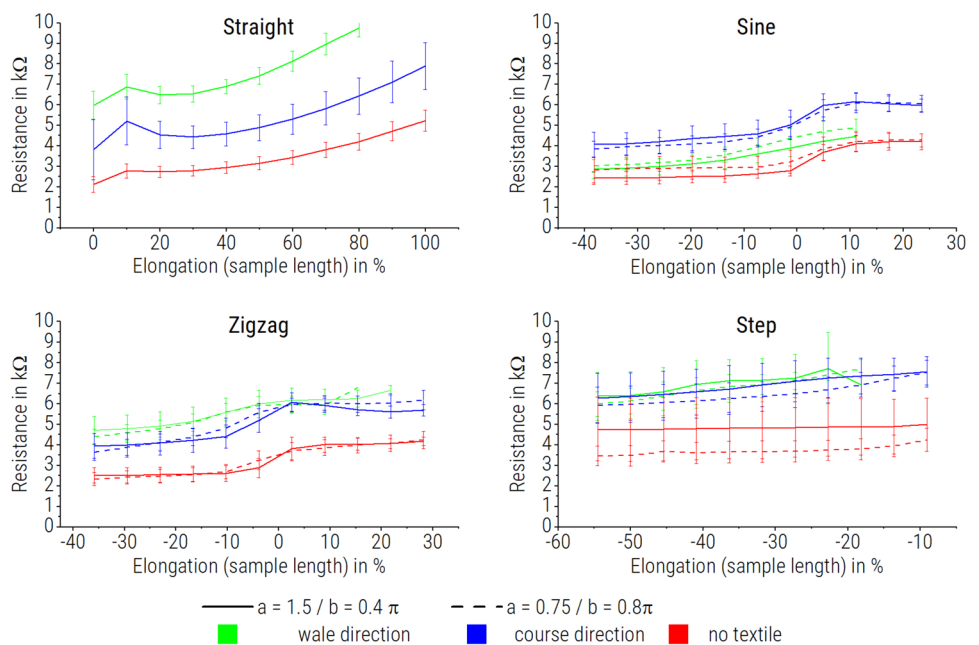
overall) show a smoother increase in resistance than the samples printed along the more stretchable course direction.

4 Discussion

4.1 Printing of conductive materials

The print factors exerting the highest influence on the resistance of 3D printed conductive polymers are infill angle, print mode and print temperature.

The fact that an infill direction parallel to the direction of conductivity measurement is preferable is not surprising, considering the assumption that internal voids and irregularities negatively affect conductivity. Other research has come to similar results [12, 15, 17, 27].

From the results for print mode (LayerByLayer vs. ObjectByObject) and to a certain degree the results for layer thickness, it can be inferred that the cooling process of the material after printing has an influence on resistivity. Pentek et al. have come to a similar conclusion for carbon-filled polylactic acid and acrylonitrile butadiene styrene, reasoning that a gentle cooling process over a long cooling time results in a more homogeneous structure [12], as it is represented in our experiments by ObjectByObject print mode. Further optimization of the cooling process might be achieved using a heated build chamber.

The results for layer thickness, while only significant for TPU15CNT, agree with previous investigations. Hohimer et al. [17], Pentek et al. [12] and Barši Palmić et al. [14] have found thicker layers to increase conductivity; Hohimer et al. have attributed this to the reduction of inter-layer faults and voids [17], Pentek et al. have ascribed this behavior to longer cooling times resulting in better homogeneity [12] and in the case of Barši Palmić et al. surface-to-volume ratio may have had an influence on the trials, as metallic fillers suffer from oxidation [14].

We observe lower resistivity with increasing print temperature; an effect that we showed to be achievable by a high nozzle temperature alone, regardless of increasing screw temperature. Waschke et al. have found similar results for materials filled with carbon-based additives and have reasoned that higher melt temperature results in reduced porosity both within the extruded strand and between two adjacent strands of material. Interestingly, in their case, the effect of increased print temperature has not been visible for a lengthwise oriented infill pattern in the case of a CNT-filler, which they have reasoned might be due to the effect of the orientation of CNT particles in the melt dominating over temperature effects [27]. Sanatgar et al. have only found an effect of print temperature on conductivity for materials with a low filler content (close to the percolation threshold), but no effect for highly filled materials. They argue

that this is because conductive filler particles are able to recover a secondary agglomerate structure that improves conductivity when the temperature is high enough; this effect is more apparent in materials with a comparatively low filler content, since secondary agglomerates form more readily and thus at lower temperatures if an excess of filler is present [11]. On the other hand, the extrusion temperature range for both experiments has varied widely: Sanatgar et al. have used Ingeo Biopolymer 6202D, which has a crystalline melt temperature of 155–170 °C and a recomended melt spinning temperature of 220–240 °C at printing temperatures of 230–260 °C, while Watschke et al. have used commercial materials with a recomended print temperature of 200–230 °C and limited their temperature experiments to 10 °C above the recomended temperature at maximum 240 °C. In our experiment, the effect of temperature is significant for the highly filled material TPU15CNT; the melting temperature of the base polymer is 180 °C and it is recomended to print at 220 °C. Our experiments are limited to a maximum of 235 °C. A higher extrusion temperature carries with it the risk of thermal damage to the polymer [2]. If the assumption of secondary agglomeration put forth by Sanatgar et al. is correct, the presumably higher shear forces as well as increased residence time above melt temperature in the extruder granulate based printers compared to filament printers could also influence this behavior.

As no comparisons for conductive materials printed with a screw-based granulate extruder exist, it is hard to quantify the influence of the difference in processing compared to a filament based printer. On the granulate printer, a wider range of print conditions lead to optically acceptable results, but conductivity is only optimal in a narrow processing window.

As Tzounis et al. [20] have used the same MWCNT as we use for TPU15CNT in this research, it is possible to draw some comparison to their achieved results. The highest filler fraction they investigated was 5%, while the material in this investigation is used as a masterbatch at 15%. Tzounis et al. have achieved a conductivity of 45.2 S/m (= 2.21 Ω cm) at 5% MWCNT-content, while our material reaches a resistivity value of 0.58 Ω cm at 15% filler content (material reistivity before printing in both cases). TPU15CNT is a masterbatch and therefore has a filler content close to the limit of printability; nevertheless, we only achieve moderate improvements in resistivity compared to the values reached by Tzounis et al.

All materials have lower conductivity after printing, which is in line with investigations on carbon-filled polylactic acid by Sanatgar et al., who have concluded that the conductive pathways between fillers are changed during the printing process [11]. However, Tzounis et al. have found little difference in conductivity before and after printing when measured in the direction of printing, but have determined cross-layer

conductivity to be slightly lower after printing. They attribute this effect to the orientation of CNT fillers during printing [20]. It is possible that the granulate extrusion process compared to filament-based printing results in a lower orientation of MWCNTs, because the screw used to push the material through the nozzle produces different shear forces. Another explanation might be found in the sample dimensions used by Tzounis et al., as their sample size of 1.6 mm × 1.6 mm using a nozzle diameter of 0.8 mm practically results in a sample consisting of two parallel lines. This is similar to the 90∞ infill orientation of the samples used in our study. Since we find the lowest resistivity in these samples, the difference between the conductivity before and after printing might have been minimized this way in the trial by Tzounis et al. Our study results imply that the conductivity of the material in filament form is not a guarantee for good conductivity of the object printed from it (object produced by 3D printing).

4.2 Response to elongation with respect to the end use in smart textiles

Previous research has heavily focused on the strain sensing capabilities of printed flexible conductive materials [10, 21, 22]. The experiments regarding elongation in this paper are made with a different goal: the use of conductive materials as conductive tracks.

Ideal strain sensors exhibit a strong and linear increase of resistance with strain, while ideal conductive tracks have minimal differences in resistance with strain. Our research shows that the resistance changes as soon as strain is applied to the material. This is even more important when the strain on a conductive track is not evenly distributed, as is the case when printing on textiles, which usually exhibit highly anisotropic elongation. It is therefore neccessary to account for the maximum elongation of the textile during use and ensure that the material of the printed track is not strained and the strain is ideally more or less uniform along the print. This can be supported by the selection and careful design of the printed conductive track.

Further research is needed to ensure stable conductivity during use since the results presented here only consider unidirectional strains. However, during use and textile care, multi-dimensional repeated stresses are expected. As washing and drying is a major issue for other smart textile technologiesp [4, 28, 29], creasing, bending and mechanical stress in general need to be taken into account.

5 Conclusion

This paper characterizes electrically conductive, elastomeric structures regarding the influence of granulate-based 3D printing parameters on their resistivity. Two commercially available materials and one custom compound are used to identify factors for the optimization of resistivity. The material with the lowest resistivity is further used for investigations into optimized shapes for 3D printing of conductive paths.

Lengthwise infill (i.e. in the direction of the conductive path) is preferable, but might not result in the best print quality and has lower mechanical resistance. Both print speed and layer thickness can be optimized for faster printing without compromising conductivity. A high print temperature is also beneficial for lowering the resistance of the finished product, but thermal degradation of the print material must be considered. If possible, a slower cooling process is preferable over rapid cooling of the printed part.

Of the three materials tested, TC80EX shows the lowest resistivity and is least influenced by small changes in the print settings. TPU15CNT can achieve good conductivity, but is more prone to changes in print factors and therefore needs more precise control of print parameters. Eel has the highest resistivity of the materials tested and is least suitable as a material for use in smart textile production. A drop in conductivity after printing is to be expected and should be taken into account during material development and compounding. If the intended function of the printed line is a conductive connection between elements of a smart textile (i.e. data transmission or energy transmission) the resistance of the material needs to remain stable when the textile is stretched. How much the conductive elements are stretched depends on the textile they are printed on and the end use of the textile. In that case, the length of the printed pathway should be ~ 10% longer than the fabric when stretched to its maximum elongation. The shape of the printed sample is most practically either a sine or zigzag pattern, while amplitude and frequency of the shape can be adapted to the practical use of the finished product (e.g. consideration of placement of the pattern).

If the printed line is to be used as a stretch sensor, desirable behavior would be a linear increase of resistance and no hysteresis. The preliminary results presented here indicate that an application of the tested materials as stretch sensors is most probably not practical.

Further research is needed before conductive paths for smart textiles can be 3D printed on textiles. Optimization of the dimensions and shapes of a conductive path as well as studies on the influence of various stress factors such as cyclic elongation, ageing, abrasion and washing are required.

Declarations

References

1. Glogowsky A (2018) 3D printed plastic/textile composites. Modifications for technical applications. In: Presentation at Dornbirn global fibre congress 2018, Dornbirn, Austria, 12 September 2018
2. Korger M, Glogowsky A, Sanduloff S, Steinem C, Huysman S, Horn B, Ernst M, Rabe M (2020) Testing thermoplastic elastomers selected as flexible three-dimensional printing materials for functional garment and technical textile applications. J Eng Fibers Fabr 15:155892502092459. https://doi.org/10.1177/1558925020924599
3. Sliz R, Huttunen O-H, Jansson E, Kemppainen J, Schroderus J, Kurkinen M, Fabritius T (2020) Reliability of R2R-printed, flexible electrodes for e-clothing applications. NPJ Flex Electron. https://doi.org/10.1038/s41528-020-0076-y
4. Yong S, Liu M, Komolafe A, Tudor J, Yang K (2021) Development of a screen-printable carbon paste to achieve washable conductive textiles. Textiles 1(3):419–432. https://doi.org/10.3390/textiles1030022
5. Li Z, Wang F, Liu L, Liu Y, Liu J, Chen X, Yao J (2022) Highly sensitive, breathable and durable e-textiles integrated by graphene ink via scalable aerodynamics assisted screen printing. Cellulose. https://doi.org/10.1007/s10570-022-04544-3
6. Angelucci A, Cavicchioli M, Cintorrino IA, Lauricella G, Rossi C, Strati S, Aliverti A (2021) Smart textiles and sensorized garments for physiological monitoring: a review of available solutions and techniques. Sensors. https://doi.org/10.3390/s21030814
7. Krinner S, Kieren M (2020) Textile-circuit—the opportunity of integrating functionality into a textile product. Commun Dev Assem Text Prod 1(1):74–79
8. Martínez-Estrada M, Gil I, Fernández-García R (2021) An alternative method to develop embroidery textile strain sensors. Textiles 1(3):504–512. https://doi.org/10.3390/textiles1030026
9. Mattmann C, Clemens F, Tröster G (2008) Sensor for measuring strain in textile. Sensors 8(6):3719–3732. https://doi.org/10.3390/s8063719
10. Georgopoulou A, Sebastian T, Clemens F (2020) Thermoplastic elastomer composite filaments for strain sensing applications extruded with a fused deposition modelling 3D printer. Flex Print Electron 5(3):035002. https://doi.org/10.1088/2058-8585/ab9a22
11. Sanatgar RH, Cayla A, Campagne C, Nierstrasz V (2019) Morphological and electrical characterization of conductive polylactic acid based nanocomposite before and after FDM 3D printing. J Appl Polym Sci 136(6):47040. https://doi.org/10.1002/app.47040
12. Pentek A, Nyitrai M, Schiffer A, Abraham H, Bene M, Molnar E, Told R, Maroti P (2020) The effect of printing parameters on electrical conductivity and mechanical properties of PLA and ABS based carbon composites in additive manufacturing of upper limb prosthetics. Crystals 10(5):398. https://doi.org/10.3390/cryst10050398
13. Gnanasekaran K, Heijmans T, van Bennekom S, Woldhuis H, Wijnia S, de With G, Friedrich H (2017) 3D printing of CNT- and graphene-based conductive polymer nanocomposites by fused deposition modeling. Appl Mater Today 9:21–28. https://doi.org/10.1016/j.apmt.2017.04.003
14. Barši Palmić T, Slavič J, Boltežar M (2020) Process parameters for FFF 3D-printed conductors for applications in sensors. Sensors. https://doi.org/10.3390/s20164542
15. Hampel B, Monshausen S, Schilling M (2017) Properties and applications of electrically conductive thermoplastics for additive manufacturing of sensors. TM Technisches Messen 84(9):593–599. https://doi.org/10.1515/teme-2016-0057
16. Zhang J, Yang B, Fu F, You F, Dong X, Dai M (2017) Resistivity and its anisotropy characterization of 3d-printed acrylonitrile butadiene styrene copolymer (ABS)/carbon black (CB) composites. Appl Sci 7(1):20. https://doi.org/10.3390/app7010020
17. Hohimer CJ, Petrossian G, Ameli A, Mo C, Pötschke P (2020) 3D printed conductive thermoplastic polyurethane/carbon nanotube composites for capacitive and piezoresistive sensing in soft pneumatic actuators. Addit Manuf 34:101281. https://doi.org/10.1016/j.addma.2020.101281
18. Eutionnat-Diffo P (2020) 3D printing of polymers onto fabric: an innovative approach to develop functional textiles. Doctoral dissertation, University of Borås
19. Eutionnat-Diffo PA, Cayla A, Chen Y, Guan J, Nierstrasz V, Campagne C (2020) Development of flexible and conductive immiscible thermoplastic/elastomer monofilament for smart textiles applications using 3D printing. Polymers. https://doi.org/10.3390/polym12102300
20. Tzounis L, Petousis M, Grammatikos S, Vidakis N (2020) 3D printed thermoelectric polyurethane/multiwalled carbon nanotube nanocomposites: a novel approach towards the fabrication of flexible and stretchable organic thermoelectrics. Materials. https://doi.org/10.3390/ma13122879
21. Xiang D, Zhang X, Li Y, Harkin-Jones E, Zheng Y, Wang L, Zhao C, Wang P (2019) Enhanced performance of 3D printed highly elastic strain sensors of carbon nanotube/thermoplastic polyurethane nanocomposites via non-covalent interactions. Compos Part B Eng 176:107250. https://doi.org/10.1016/j.compositesb.2019.107250
22. Xiang D, Zhang X, Harkin-Jones E, Zhu W, Zhou Z, Shen Y, Li Y, Zhao C, Wang P (2020) Synergistic effects of hybrid conductive nanofillers on the performance of 3D printed highly elastic strain sensors. Compos Part A. https://doi.org/10.1016/j.compositesa.2019.105730
23. Osswald T, Baur E, Brinkmann S, Oberbach K, Schmachtenberg E (2006) International plastics handbook: the resource for plastics engineers, 4th edn. Hanser, Munich
24. Gorlachova M, Mahltig B (2021) 3D-printing on textiles—an investigation on adhesion properties of the produced composite materials. J Polym Res. https://doi.org/10.1007/s10965-021-02567-1

25. Korger M, Bergschneider J, Lutz M, Mahltig B, Finsterbusch K, Rabe M (2016) Possible applications of 3D printing technology on textile substrates. IOP Conf Ser Mater Sci Eng 141:012011. https://doi.org/10.1088/1757-899X/141/1/012011

26. Meyer P, Döpke C, Ehrmann A (2019) Improving adhesion of three-dimensional printed objects on textile fabrics by polymer coating. J Eng Fibers Fabr 14:155892501989525. https://doi.org/10.1177/1558925019895257

27. Watschke H, Hilbig K, Vietor T (2019) Design and characterization of electrically conductive structures additively manufactured by material extrusion. Appl Sci 9(4):779. https://doi.org/10.3390/app9040779

28. Mamun MAA, Islam MT, Islam MM, Sowrov K, Hossain MA, Ahmed DM, Shahariar H (2020) Scalable process to develop durable conductive cotton fabric. Adv Fiber Mater 2(6):291–301. https://doi.org/10.1007/s42765-020-00051-x

29. Liu W, Shangguan D, Lee JC (2020) Evaluation of launderability of electrically conductive fabrics for e-textile applications. IEEE Trans Compon Packag Manuf Technol 10(5):763–769. https://doi.org/10.1109/TCPMT.2020.2981902